https://doi.org/10.46813/2022-137-064

RELATIVE LENGTH AS A CLASSIFICATION PARAMETER OF THE CRYSTALLIZATION MODE OF AMORPHOUS FILMS

A.G. Bagmut
National Technical University "Kharkiv Polytechnic Institute", Kharkiv, Ukraine
E-mail: agbagmut@gmail.com

The possibility of using of the relative length δ_0 as a parameter, determining the polymorphous crystallization mode of amorphous films, was considered. Following polymorphous crystallization modes have been identified based on the structural and morphological characteristics. Layer polymorphous crystallization mode, describes the nucleation and growth of a single-crystal layer in the field of the electron-beam impact, for which δ_0 is about several thousand (3000…5000). Island polymorphous crystallization mode, describes the nucleation and growth of a polycrystalline layer, for which δ_0 is about several hundred (100…1100). Dendrite polymorphous crystallization mode, describes the nucleation and growth of dendrite, for which δ_0 is about several thousand (~ 4000).

PACS: 61.14.−x, 61.43.Dq, 61.72.Cc, 64.70.Kb, 68.37.Lp, 68.55.A−, 68.37.−d

INTRODUCTION

Crystallization mode is a function of free energy of various phases and of concentration of chemical elements. It can take place with following reactions [1]: 1. Polymorphous crystallization, whereas an amorphous substance transforms into crystalline without the change in composition. It is typical both for pure elements and for stoichiometric chemical compounds. 2. Preferred crystallization of one of the phases during the first process stage and the following crystallization of matrix on the second stage. 3. Eutectic crystallization in which an almost spontaneous formation of two crystalline phases takes place.

The phenomenological scheme, based on numerous TEM studies, suggests the following polymorphous crystallization modes [2]. 1. Layer polymorphous crystallization (LPC). By analogy with Bauer criterion [3], this type can bi realized when the inequality $\sigma_a \geq \sigma_c+\sigma_{ac}+\varepsilon_d$ is satisfied. Here σ_a, σ_c, σ_{ac} are the surface energy of amorphous phase-vacuum interface, of the crystalline phase-vacuum interface and surface energy of the amorphous-crystalline phase interface respectively. ε_d is the energy of deformation of the growing crystalline layer. 2. Island polymorphous crystallization (IPC). This type is realized when the opposite inequality $\sigma_a \leq \sigma_c+\sigma_{ac}+\varepsilon_d$ is satisfied. 3. Dendrite polymorphous crystallization (DPC). This type is realized when initially $\sigma_a \geq \sigma_c+\sigma_{ac}+\varepsilon_d$, and after critical dimension of a crystal, when $\sigma_a \leq \sigma_c+\sigma_{ac}+\varepsilon_d$.

Quantification of the crystallization mode (LPC, DPC ore IPC) can be done on the basis of the value of relative length δ_0, defined as

$$\delta_0 = \frac{D_0}{a_0}, \quad (1)$$

in the case of LPC, and as

$$\delta_0 = \frac{D_0}{\sqrt[3]{\Omega}} \quad (2)$$

in the case of IPC and DPC [4]. Characteristic unit length D_0 is the crystal size at time t_0, after which the volume of the amorphous phase decreases by a factor of e = 2.718. a_0 is a cell parameter of a growing crystal. Ω is the volume of the unit cell of a growing crystal. The difference in the determination of δ_0 is due to the fact, that in the case of LPC a single crystal (with a cell parameter a_0) is formed in the investigated region, and in the case of IPC (or DPC) a polycrystalline film (or dendrite), whose grains have different orientations.

The purpose of this work was to classify the available data on the electron-beam crystallization of amorphous films depending on the relative length δ_0.

EXPERIMENTAL SECTION

Amorphous films were prepared with methods of laser, thermal and ion-plasma deposition on substrates of (001) KCl at room temperature. Its crystallization was initiated by electron beam irradiation in the column of a transmission electron microscope (TEM). The crystallization rate was controlled by varying the density of the electron current through the sample, which was varied with the electron beam focusing. Its structure was investigated by the electron diffraction and TEM methods "in situ". The experimental electron-diffraction data were compared with the JCPDS Powder Diffraction File (International Centre for Diffraction Data, Swarthmore, PA, 1996) [5].

The process of crystallization of a film was recorded from the screen of an electron microscope at a frame rate of 30 s^{-1}. Data on the kinetics of the crystallization process were obtained from the analysis of individual frames of the video recorded "in situ" at a fixed tangential crystal growth rate v, which is determined by the relationship

$$v = \frac{\Delta D}{\Delta t}. \quad (3)$$

In expression (3) ΔD is the increment in the average value of the dimension D of microcrystals during a time period Δt between the two video frames, corresponding to the moments of the recording t and $t+\Delta t$.

RESULTS AND DISCUSSION

LAYER CRYSTALLIZATION MODE

In the case of LPC in the region of investigation a single flat crystal nucleates and grows at a rate v. Usually crystal has the shape of a disk (Fig. 1). By the time t_0 the crystal in the film plane has the size $D_0 = vt_0$.

The increase in the diameter of the disk can be represented as the sequential attachment of unit cells to the crystal–amorphous phase interface. In this case, according to (1), the relative length δ_0 is equal to the number of lattice parameters a_0, which fit within the interval equal to D_0.

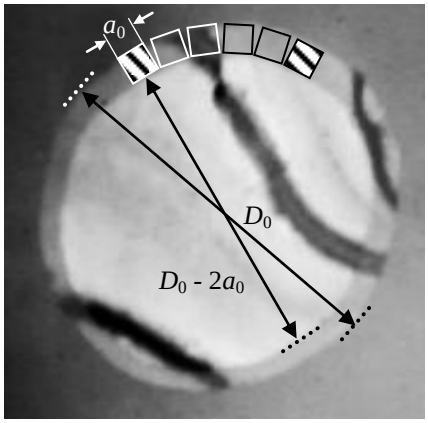

Fig. 1. Schematic diagram of the crystal growth according to the layer polymorphic crystallization mechanism. Shaded squares correspond to projections of the unit cells onto the figure plane. The illustration is based on the growth of a disk-shaped crystal in amorphous film of Ta_2O_5

TEM images and selected area electron diffraction (SAED) patterns of disc-shape crystals of V_2O_3, Cr_2O_3, and Ta_2O_5 are presented in Fig. 2 respectively. Based on the frame-by-frame analysis of the video frames of the crystallization process, the kinetic curves of crystal growth in amorphous films were plotted.

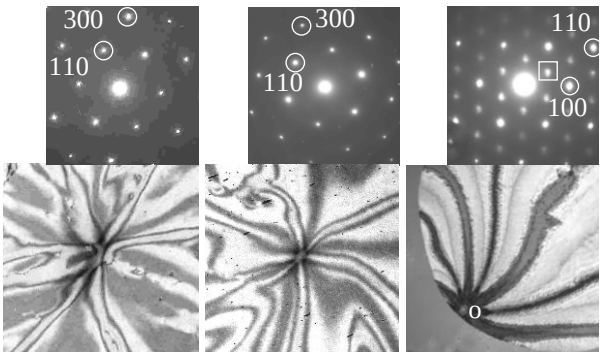

Fig. 2. TEM images and SAED patterns of disc-shape V_2O_3 (a), Cr_2O_3 (b), and Ta_2O_5 (c) crystals, growing in amorphous films under the influence of electron irradiation

The dependence on time t of the diameters D for disc-shape V_2O_3 (straight 1), Cr_2O_3 (straight 2), and Ta_2O_5 (straight 3) crystals are shown in Fig. 3,a. Lines were plotted by the data of D measurements using the least-squares technique. Linear dependence $D(t)$ takes place:

$$D = 0.235\ t + 0.054\ \mu m, \quad (4a)$$

$$D = 0.179\ t - 0.085\ \mu m, \quad (4b)$$

$$D = 0.120\ t + 0.037\ \mu m \quad (4c)$$

for V_2O_3 (4a), Cr_2O_3 (4b), and Ta_2O_5 (4c) respectively. According to (4a), (4b), and (4c) the tangential crystal growth rate v_τ (defined as the derivative of the crystal diameter with time D'_t) is 0.235; 0.179, and 0.120 μm·s^{-1} for V_2O_3, Cr_2O_3, and Ta_2O_5 respectively. These data are shown in Table 1.

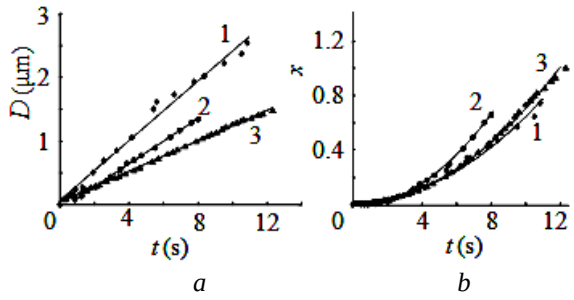

Fig. 3. The dependence on time of the crystal diameter D(t) (a) and of the crystals fraction x(t) (b). Lines 1, 2, and 3 corresponds to the crystallization of amorphous films of V_2O_3, Cr_2O_3 and Ta_2O_5 respectively

The dependences on time of the crystallization fraction $x(t)$ are shown in Fig. 3b. A quadratic relation takes place:

$$x = 0.006\ t^2 + 0.022, \quad (5a)$$

$$x = 0.011\ t^2 - 0.015, \quad (5b)$$

$$x = 0.007\ t^2 + 0.011 \quad (5c)$$

for V_2O_3 (5a), Cr_2O_3 (5b), and Ta_2O_5 (5c) respectively. When $x = 0.632$, according to (5a)–(5c) characteristic unit of time $t_0 = 10.08$; 61.89, and 9.42 s for V_2O_3, Cr_2O_3, and Ta_2O_5 respectively (Table 2). The values of D_0 and t_0 are related by the relation

$$D_0 = v_\tau \cdot t_0. \quad (6)$$

The values of D_0, calculated according to (6), are given in Table 1.

Crystals of V_2O_3 and Cr_2O_3 belong to the rhombohedra structure with space group $R\bar{3}c$. In terms of hexagonal structure for V_2O_3 lattice parameters a_0 = 0.4920 nm and c_0 = 1.3883 nm (JCPDS 26-0278 [5]). For Cr_2O_3 lattice parameters a_0 = 0.4958 nm and c_0 = 1.3593 nm (JCPDS 06-0504 [5]). For crystals of V_2O_3 and Cr_2O_3 with the [001] zone axis (see Fig. 2,a,b) the projection of the unit cell on the plane of the film is a rhomb with a side a_0 and apex of 120°. In this case δ_0 is the number of cell parameters a_0, stacked at a distance, equal to D_0. According to (1) for V_2O_3 the relative length $\delta_0 \approx 4817$ and for Cr_2O_3 $\delta_0 \approx 2763$ (see Table 1).

SAED pattern of the area near the point "o" (see Fig. 2,c) corresponds to the (001) section of the reciprocal lattice of Ta_2O_5. The observed diffraction peaks can be ascribed as the hexagonal phase of δ-Ta_2O_5 with unit cell parameters a_0 = 0.3624 nm and c_0 = 0.3880 nm (JCPDS 19-1299). A detailed analysis of such electron diffraction patterns is given in [6, 7]. Crystallization of the amorphous film is accompanied by the ordering of oxygen vacancies. In this case, a superstructure lattice is formed, which is also hexagonal. It has parameters $a_s = \sqrt{3}a_0$, $c_s = c_0$ and is rotated with respect to the base lattice by 30°. In this SAED pattern the reflections of the main and superstructure lattice are marked with circles and squares respectively. The relative length δ_0, which

according to (1) is the ratio of D_0 to a_0, is equal to 3118 (see Table 1).

Table 1

Parameters of the LPC of amorphous films*

Parameter	V_2O_3	Cr_2O_3	Ta_2O_5	Sb_2S_3
v_τ, μm·s^{-1}	0.235	0.179	0.120	0.087
t_0, s	10.08	7.67	9.42	17.546
D_0, μm	2.37	1.37	1.13	1.53
δ_0	4817	2763	3118	4992

*v_τ, is the tangential growth rate of crystals, t_0 is the characteristic time unit, D_0 is the characteristic length unit, δ_0 is the relative length.

Fig. 4 illustrates polymorphous crystallization of amorphous film of Sb_2S_3. Film was obtained by thermal evaporation of a substance in vacuum on (001) KCl at room temperature. TEM images of a video tape of elliptical crystal growth are shown. Based on the frame-by-frame analysis of the video frames of the crystallization process, the kinetic curves of crystal growth in amorphous films were plotted (Fig. 5). The dependence on time of the length of the major axis 2OA and minor axis 2OB (see Fig. 4,b) of the ellipse-shaped Sb_2S_3 crystal are shown in Fig. 5,a. A linear dependence takes place:

$$2OA = 0.087t + 0.059 \text{ μm}, \quad (7a)$$

$$2OB = 0.043t + 0.020 \text{ μm}. \quad (7b)$$

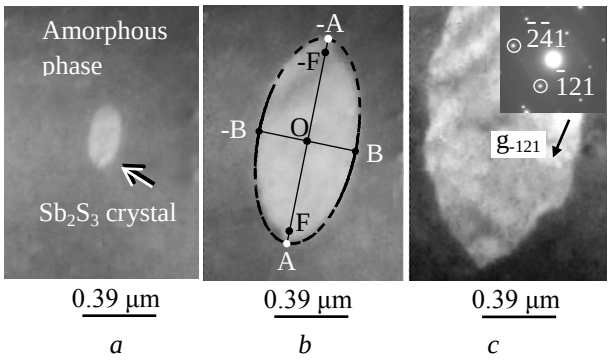

Fig. 4. Polymorphous crystallization of amorphous film of Sb_2S_3. Electron microphotographs correspond to the frames at the time moment t, which have passed from the beginning of the recording of the crystallization process: a – t = 3.63 s; b – t = 11.87 s; c – t = 19.50 s. SAED pattern of the crystalline Sb_2S_3 is shown in the upper right corner of the frame 4c. The dotted line marks the ellipse with eccentricity 0.881

According to (7a) the growth rate v_{2OA} of the major axis 2OA (the tangent of the angle of inclination of the line to the abscissa axis) is equal to 0.087 μm·s^{-1} (see Table 1). The growth rate v_{2OB} of the minor axis 2OB is half as much and is equal to 0.043 μm·s^{-1}.

The dependences on time of the crystallization fraction $x(t)$ in coordinates of x - t^2 are shown in Fig. 5,b. A quadratic relation takes place:

$$x = 0.002t^2 + 0.017. \quad (8)$$

According to (8), the value $x = 0.632$ corresponds to the characteristic time $t = t_0 = 17.54$ s. Substituting this value to (6) for $\langle v_\tau \rangle = v_{2OA} = 0.087$ μm·s^{-1} we get $2OA \approx D_0 = 1.53$ μm (see Table 1).

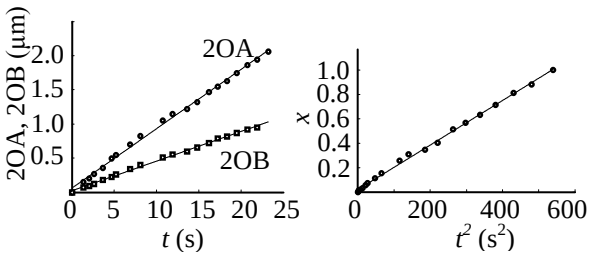

Fig. 5. Kinetics of the polymorphous crystallization of amorphous film of Sb_2S_3: a – time dependence of the length of the major axis 2OA and minor axis 2OB of the ellipse-shaped Sb_2S_3 crystal; b – time dependence of the crystals fraction x(t)

In the crystalline state Sb_2S_3 has an orthorhombic lattice with periods $a = 1.123$ nm, $b = 1.131$ nm, and $c = 0.3841$ nm (JCPDS 42-1393 [5]). The SAED pattern of the Sb_2S_3 crystal (see Fig. 4,c) sets the position of the diffraction vector $g_{\bar{1}21}$. In this direction, the increasing of the major axis 2OA of the ellipse-shaped Sb_2S_3 crystal takes place. This is done by attaching of $(\bar{1}21)$ planes with the interplanar distance $d_{\bar{1}21} = 0.3057$ nm. Then, according to (1), using $d_{\bar{1}21}$ instead of a_0, we get the relative length $\delta_0 \approx 4992$ (see Table 1).

ISLAND CRYSTALLIZATION MODE

TEM images and electron diffraction patterns of partially crystallized films of ZrO_2 (ion-plasma evaporation), ZrO_2 (laser evaporation), and Yb_2O_2S (electron beam evaporation) are presented in Fig. 6 respectively. Based on the frame-by-frame analysis of the video frames of the crystallization process, the kinetic curves of crystal growth in amorphous films were plotted.

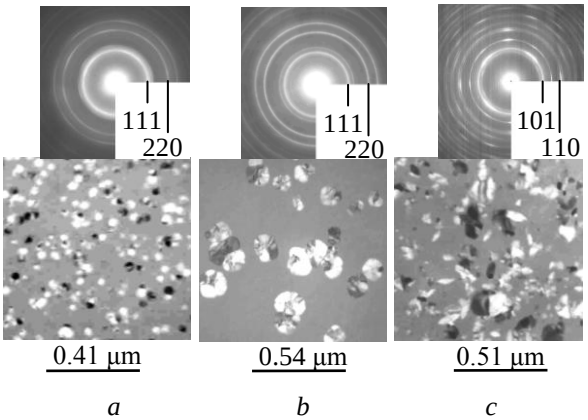

Fig. 6. TEM images and electron diffraction patterns of partially crystallized films of ZrO_2 (ion-plasma evaporation) (a), ZrO_2 (laser evaporation) (b), and Yb_2O_2S (electron beam evaporation) (c), growing in amorphous films under the influence of electron irradiation

The dependence on time of the average diameter $\langle D \rangle$ of crystals are shown in Fig. 7,a. Line 1 corresponds to ZrO_2 (ion-plasma evaporation), line 2 corresponds to ZrO_2 (laser evaporation), and line 3

corresponds to Yb_2O_2S (electron beam evaporation). Linear dependence <*D*> (*t*) takes place:

$$<D> = 0.012 \cdot t + 0.007 \text{ μm}, \quad (9a)$$

$$<D> = 0.120 \cdot t + 0.009 \text{ μm}, \quad (9b)$$

$$<D> = 0.297 \cdot t + 0.150 \text{ μm} \quad (9c)$$

for ZrO_2 (ion-plasma evaporation) (9a), ZrO_2 (laser evaporation) (9b), and Yb_2O_2S (electron beam evaporation) (9c) respectively.

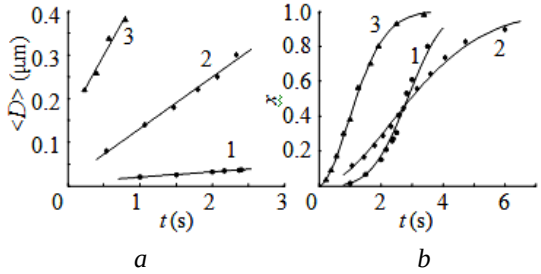

Fig. 7. The dependence on time of the average crystal diameter <D>(t) (a) and of the crystals fraction x(t) (b). Lines 1, 2, and 3 corresponds to the crystallization of amorphous films of ZrO_2 (ion-plasma evaporation), ZrO_2 (laser evaporation), and Yb_2O_2S (electron beam evaporation) respectively

According to (9a), (9b), and (9c) the tangential crystal growth rate v_τ is 0.012; 0.120, and 0.297 μm·s^{-1} for ZrO_2 (ion-plasma evaporation), ZrO_2 (laser evaporation), and Yb_2O_2S (electron beam evaporation) respectively. These data are shown in Table 2.

The dependences on time of the crystallization fraction $x(t)$ are shown in Fig. 7,b. An exponential relation takes place:

$$x = 1 - \exp(-0.015 \cdot t^{3.6}), \quad (10a)$$

$$x = 1 - \exp(-0.097 \cdot t^{1.8}), \quad (10b)$$

$$x = 1 - \exp(-0.5 \cdot t^{1.8}) \quad (10c)$$

for ZrO_2 (ion-plasma evaporation), ZrO_2 (laser evaporation) and Yb_2O_2S (electron beam evaporation) respectively. When $x = 0.632$, according to (10a)–(10c) characteristic unit of time t_0 = 3.21; 3.65, and 1.47 s for ZrO_2 (ion-plasma evaporation), 441 and Yb_2O_2S (electron beam evaporation) respectively. The values t_0 and D_0, calculated according to (6), are given in Table 2.

Table 2

Parameters of the IPC of amorphous films

Parameter	ZrO_2 ion-plasma evaporation	ZrO_2 laser evaporation	Yb_2O_2S electron beam evaporation
v_τ, μm·s^{-1}	0.012	0.120	0.297
t_0, s	3.21	3.65	1.47
D_0, μm	0.04	0.44	0.44
δ_0	79	441	1030

Crystals of ZrO_2 belong to the cubic structure with space group Fm3m with the unit cell parameter a_0 = 0.509 nm and volume $\Omega = 0.13187$ nm^3 (JCPDS 27-0997 [5]). The relative length δ_0, which according to (2) is the ratio of D_0 to $\Omega^{1/3}$ is equal to 79 for ZrO_2 (ion-plasma evaporation) and to 441 for ZrO_2 (laser evaporation) (see Table 2).

Lattice parameters of crystals of hexagonal modification of Yb_2O_2S (ytterbium oxide sulfide) are as follows: $a_0 = 0.3722$ nm, $c_0 = 0.6496$ nm, and $\Omega = 0.07793$ nm^3 (JCPDS 26-0614 [5]). The relative length δ_0, which according to (2) is the ratio of D_0 to $\Omega^{1/3}$ is equal to 1030 (see Table 2).

DENDRIT CRYSTALLIZATION MODE

Fig. 8 illustrates dendrite crystallization of amorphous film of HfO_2. Film was obtained by laser evaporation of Hf target in an oxygen atmosphere on (001) KCl at room temperature. TEM images of a video of dendrite growth are shown in Fig. 8,a–c. Point O is the site of the formation of first-order dendrite branches. These branches are located inside the AOB and COD sectors. The branches of the second and higher orders are located inside the BOC ore AOD sectors, having at the vertex at the point O the angle ≈ 130° (see Fig. 8,c).

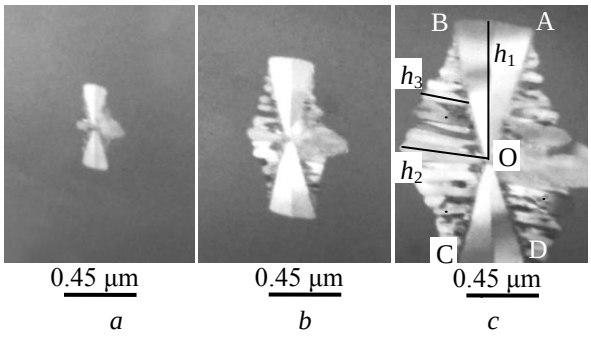

Fig. 8. Dendrite crystallization of amorphous film of HfO_2. Electron microphotographs correspond to the frames at the time moment t, which have passed from the beginning of the recording of the crystallization process: a – t = 5.67 s; b – t = 9.70 s; c – t = 15.67 s

Based on the frame-by-frame analysis of the video of the crystallization process, the kinetic curves of dendrite growth in amorphous films were plotted. Fig. 9,a shows the dependence of the length h_1 of the first order dendrite branch and of the length h_2 and h_3 of the second order dendrite branches on time t (see Fig. 8,c). The increase of h_1, h_2, and h_3 occurs at a constant rate $v_1 = 0.064$ μm·s^{-1}, $v_2 = 0.041$ μm·s^{-1}, $v_3 = 0.040$ μm·s^{-1} respectively. The ratio $v_1 > v_2 > v_3$ shows, that the dendrite branches of the first order grow faster than all.

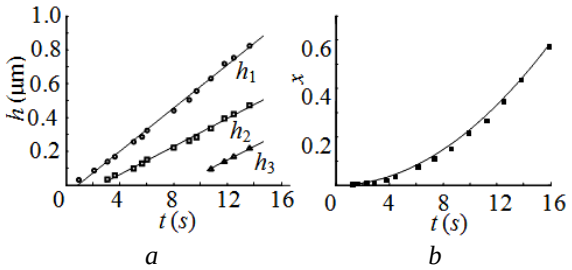

Fig. 9. Kinetic growth curves of dendrite of monoclinic modification of HfO_2 in amorphous film, constructed in accordance with the frames of the film in Fig. 8. The dependence on time of the dendrite branches length h_1, h_2, h_3 (a). The dependence on time of the crystals fraction x(t) (b)

The dependence on time of the HfO_2 crystals fraction is shown in Fig. 9,b. A quadratic relation takes place:

$$x = 0.0026\, t^2 - 0.001. \quad (11)$$

When $x = 0.632$, according to (11) characteristic unit of time $t_0 = 15.5$ s. Whereas the growth rate of the dendrite $v_\tau = 2v_1$, we get the value $D_0 = 2v_1 t_0 = 1.98$ μm. Lattice parameters of HfO_2 crystals of monoclinic modification are as follows: $a_0 = 0.51157$ nm; $b_0 = 0.51819$ nm; $c_0 = 0.52851$ nm; $\beta = 99.259°$, and $\Omega = 1.3828 \cdot 10^{-10}$ μm^3 (JCPDS 43-1017 [5]). The relative length δ_0, which according to (2) is the ratio of D_0 to $\Omega^{1/3}$ is equal to 3829 (Table 3).

Table 3

Parameters of the DPC of amorphous films of HfO_2

v_τ, μm·s^{-1}	t_0, s	D_0, μm	δ_0
0.128	15.5	1.98	3829

CONCLUSIONS

The available data, concerning the electron-beam crystallization of amorphous films, are classified by structural and morphological characteristics (qualitatively) and by the numerical value of the relative length δ_0 (quantitatively). Following polymorphous crystallization modes have been identified.

1. LPC, describes the nucleation and growth of a single-crystal layer in the field of the electron-beam impact, for which δ_0 is about several thousand (3000…5000). Crystals in an amorphous film grow in the tangential direction at a constant rate. Time dependence of the fraction of the crystallized region is quadratic.

2. IPC, describes the nucleation and growth of a polycrystalline layer, for which δ_0 is about several hundred (100…1100). The dependence on time of the average crystal diameter is linear. Time dependence of the fraction of the crystallized region is exponential.

3. DPC mode describes the nucleation and growth of dendrite, for which δ_0 is about several thousand (~ 4000). The dependence on time of the dendrite branches length is linear and of the fraction of the crystallized region is quadratic.

REFERENCES

1. U. Köster, U. Herold. *Crystallization of metallic glasses* / H.-J. Güntherodt**,** H. Beck (Eds.). *Glassy Metals*. I. *Ionic Structure, Electronic Transport, and Crystallization*. New York: "Springer", 1981, p. 225-259.

2. A.G. Bagmut. Layer, island and dendrite crystallizations of amorphous films as analogs of Frank-van der Merwe, Volmer-Weber and Stranski-Krastanov growth modes // *Functional Materials*. 2019, v. 26, p. 6-15.

3. E. Bauer, H. Poppa. Recent advances in epitaxy // *Thin Solid Films*. 1972, v. 12, p. 187-185.

4. A.G. Bagmut, I.A. Bagmut. Kinetics of electron beam crystallization of amorphous films of Yb_2O_2S // *Journal of Non-Crystalline Solids*. 2020, v. 547, p. 120286-120292.

5. JCPDS Powder Diffraction File (International Centre for Diffraction Data, Swarthmore, PA, 1996).

6. J. Spyridelis, P. Delavignette, S. Amelinckx. On the Superstructures of Ta_2O_5 and Nb_2O_5 // *Phys. Stat. Sol*. 1967, v. 19, p. 683-704.

7. В.М. Косевич, А.А. Сокол, Ю.П. Дьяконенко. Особенности электронограмм кристаллов Nb_2O_5 с длиннопериодной сдвиговой сверхструктурой // *Кристаллография*. 1983, т. 28, с. 483-487.

Article received 12.05.2021

ОТНОСИТЕЛЬНАЯ ДЛИНА КАК КЛАССИФИКАЦИОННЫЙ ПАРАМЕТР КРИСТАЛЛИЗАЦИОННЫХ МОД В АМОРФНЫХ ПЛЕНКАХ

А.Г. Багмут

Рассмотрена возможность использования относительной длины δ_0 в качестве параметра, определяющего тип полиморфной кристаллизации аморфных пленок. Были идентифицированы следующие типы полиморфной кристаллизации на основе структурных и морфологических характеристик. Слоевая полиморфная кристаллизация описывает зарождение и рост монокристаллического слоя в поле электронно-лучевого воздействия. Для нее δ_0 составляет нескольких тысяч (3000…5000). Островковая полиморфная кристаллизация описывает зарождение и рост поликристаллического слоя. Значение δ_0 составляет несколько сотен (100…1100). Дендритная полиморфная кристаллизация описывает зарождение и рост дендрита. В этом случае δ_0 составляет несколько тысяч (~ 4000).

ВІДНОСНА ДОВЖИНА ЯК КЛАСИФІКАЦІЙНИЙ ПАРАМЕТР КРИСТАЛІЗАЦІЙНИХ МОД АМОРФНИХ ПЛІВОК

О.Г. Багмут

Розглянуто можливість використання відносної довжини δ_0 як параметр, що визначає тип поліморфної кристалізації аморфних плівок. Були ідентифіковані наступні типи поліморфної кристалізації на основі структурних і морфологічних характеристик. Це шарова поліморфна кристалізація, яка описує зародження і зростання монокристалічного шару в полі електронно-променевого впливу. Для неї δ_0 становить кількох тисяч (3000…5000). Острівцева поліморфна кристалізація описує зародження і зростання полікристалічного шару. Значення δ_0 становить кількох сотень (100…1100). Дендритна поліморфна кристалізація описує зародження і зростання дендриту. В цьому випадку δ_0 складає кілька тисяч (~ 4000).